Materiales de Construcción (74) 356
October-December 2024, e355
ISSN-L: 0465-2746, eISSN: 1988-3226
https://doi.org/10.3989/mc.2024.390224

A review of five years' experience on the effect of fibers on the autogenous healing of Ultra High-Performance Fiber-Reinforced Concrete

M. Roig-Flores [a]✉, H. Doostkami [a,b], P. Serna [b]

a. Department of Mechanical Engineering and Construction, Universitat Jaume I (Castelló de la Plana, Spain)
b. Institute of Concrete Science and Technology (ICITECH), Universitat Politècnica de València (València, Spain)
✉: roigma@uji.es

Received 18 July 2024
Accepted 29 September 2024
Available on line 10 January 2025

ABSTRACT: Ultra High-Performance Fiber Reinforced Concrete (UHPFRC) is known for its enhanced self-healing abilities, attributed to its low water-to-cement ratio, high content of un-hydrated cement particles, and multi-cracking pattern. This study investigates the effect of different fiber types and contents on UHPFRC self-healing. Two UHPFRC mixes were evaluated: one with 65/35 3D steel fibers in a dosage of 40 kg/m³ and another with short straight-shaped steel fibers (13/0.2) in a dosage of 160 kg/m³. The self-healing performance was evaluated through crack closure and water permeability. In addition, resistance to chloride penetration was evaluated in healed cracks. Pre-cracked disk specimens with cracks between 100-450 µm were subjected to two healing conditions: water immersion at 20°C and exposure to a humidity chamber (20°C, 95% RH). The mix with higher fiber content (U160) obtained superior crack closure and healing efficiency, particularly under water immersion. For cracks smaller than 150 µm, U160 achieved nearly complete healing, while U40 achieved limited healing efficiency. In addition, water permeability and chloride penetration tests revealed that the U160 mix offered higher resistance to water and chloride penetration, emphasizing the role of fiber content and crack pattern in improving the self-healing and durability of UHPFRC.

KEY WORDS: Chloride penetration; Cracking; Self-healing; Ultra High-Performance Fiber Reinforced Concrete; Water permeability.

Citation/Citar como: Roig-Flores M, Doostkami H, Serna P. 2024. A review of five years' experience on the effect of fibers on the autogenous healing of Ultra High-Performance Fiber-Reinforced Concrete. Mater. Construcc. 74(356):e355. https://doi.org/10.3989/mc.2024.390224.

RESUMEN: *Efecto de las fibras en el autosanado de un Hormigón de Ultra Altas Prestaciones.* El hormigón de ultra altas prestaciones reforzado con fibras (UHPFRC) es conocido por sus capacidades mejoradas de autosanado, atribuidas a su baja relación a/c, alto contenido en partículas de cemento sin hidratar y un patrón de fisuración múltiple. Este estudio investiga el efecto de diferentes contenidos y tipos de fibras en las capacidades de autosanado del UHPFRC. Se evaluaron dos amasadas de UHPFRC: una con 40 kg/m³ de fibras de acero 3D 65/35 y otra con 160 kg/m³ de microfibras de acero (13/0.2). La capacidad de autosanado se evaluó mediante el cierre de fisuras y permeabilidad al agua. Además, se estudió la resistencia a la penetración de cloruros en los elementos tras el autosanado. Las probetas ensayadas con fisuras entre 100-450 µm fueron sometidos a dos condiciones de sanado diferentes: inmersión en agua a 20°C y cámara de humedad (20°C, 95% RH). La serie con mayor contenido de fibra (U160) obtuvo una capacidad de autosanado superior, tanto en cierre de fisura como en permeabilidad, especialmente para probetas sanadas en inmersión en agua. Para fisuras por debajo de 150 µm, la serie U160 logró un autosanado casi completo, mientras que la mezcla U40 obtuvo una eficiencia limitada. Tras el proceso de autosanado, la serie U160 obtuvo mayor resistencia frente a la penetración de agua y cloruros, resaltando el papel del contenido de fibras en la mejora de la autosanado y durabilidad del UHPFRC.

PALABRAS CLAVE: Autosanado; Fisuración; Hormigón de Ultra Altas Prestaciones; Penetración de cloruros; Permeabilidad al agua.

1. INTRODUCTION

Self-healing materials possess the ability to repair damage autonomously or with minimal external intervention. In construction, the use of self-healing materials is expected to enhance the longevity of structures and reduce maintenance and repair needs (1). Reinforced concrete structures often experience small cracks (less than 0.3 mm) due to the material's low tensile strength, and such cracks are considered normal in many structures, as specified in Eurocode 2. Concrete has a natural self-healing ability, known as autogenous healing, which allows it to seal small cracks through ongoing hydration and carbonation processes (1). The healing process has been known for years, especially in concrete water reservoirs and pipes, where crack sealing and leakage stop were detected. The first mention to the phenomena is usually attributed to the French Academy of Sciences (1, 2). Well-known technical books also described the phenomena with different names, such as "*cicatrization*" in (3), and is always attributed to cracks below 0.2-0.3 mm, and thus, within the allowable crack width values.

Concrete autogenous healing is typically disregarded in the design of typical concrete structures, but it is considered in Eurocode 2 in part 3, EN 1992-3 "Liquid retaining and containment structures", which relates to design of watertight concrete structures, usually exposed to one-sided water pressure (such as basements, tunnels and water tanks). EN 1992-3 allows certain crack width values for tightness class 1, depending on the water pressure and thickness of the reinforced concrete wall, with values generally between 0.05 and 0.2 mm, given the requirement that sealing of the cracks would occur in a short-time, which, however, is not always guaranteed.

Recent research has focused on improving autogenous healing (4, 5), designing specialized products to promote self-healing (autonomous healing) (1, 6), or better understanding these processes. It has been widely reported that the visual closure of cracks does not always guarantee improved durability (7, 8), making the study of self-healing in terms of transport properties crucial.

From the three mechanisms involved in the transport of fluids, permeability, diffusion, and sorption (9), the most relevant mechanism will be different depending on the specific civil work and its contact with water. There are several civil constructions where permeability is the main mechanism with different range of values of water pressure, such as dams (~50-100 meters of water column, mWc), water reservoirs (1-2), concrete pipes (0.5-1 mWc) or even variable mWc in the case of the groundwater level, a situation that can be found in many foundations or constructions under the ground level such as a parking.

Traditionally, concrete permeability has been evaluated in the uncracked state following EN 12390-8. This approach enables the assessment of water penetration depth and whether it reaches the reinforcement. In specimens with cracks, the flow of fluid through the sample under a specific pressure can be evaluated. Testing methods for cracked or damaged samples are quite similar to those used for porous materials in fields like soil mechanics or hydrogeology, where

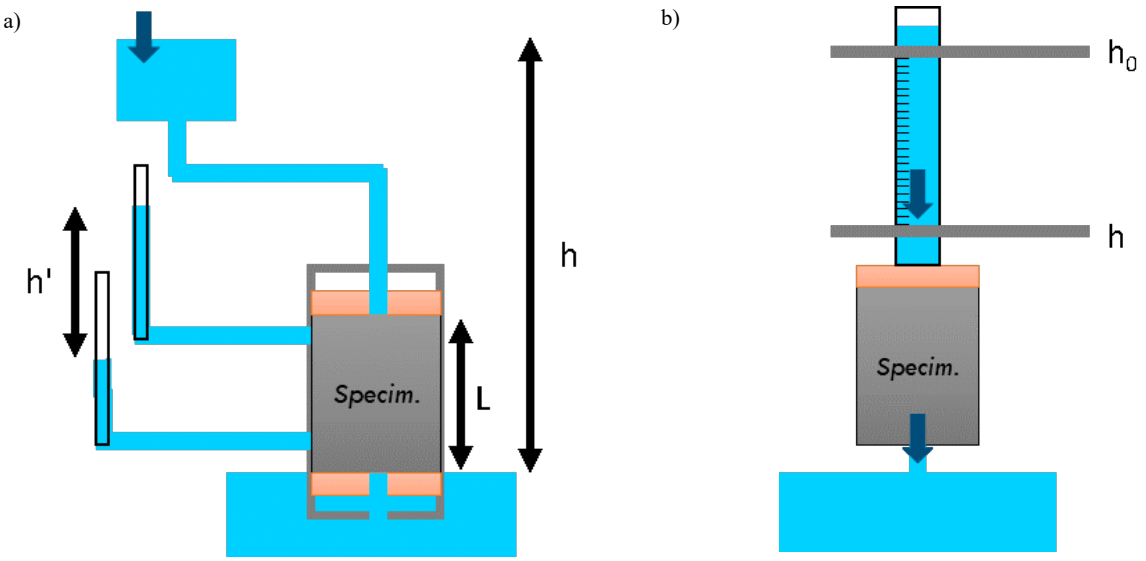

Figure 1. Different setups for testing water permeability in soils, a) constant head water permeability and b) falling head water permeability.

fluid flow is measured using either the constant head or falling head methods (figure 1). From these tests, a permeability coefficient (k) is estimated using Darcy's law, with slightly different equation depending on the type of test. However, it should be mentioned, that Darcy's law was formulated for porous mediums and its applicability may be limited in concreted cracked specimens where other phenomena (such as turbulences) may occur. Other classifications on the type of permeability tests can be found in the literature (10), such as a differentiation between discrete tests (healing occurs between tests) and continuous permeability tests (where healing occurs simultaneously to the test).

For the evaluation of self-healing through transport properties, there is a need of inducing a previous damage (usually a crack), unlike with mechanical tests. Usually, water permeability in cracked conditions is measured after inducing these cracks.

Previous authors (4) designed a test apparatus capable of inducing tensile cracks in concrete samples and assessing water permeability under varying pressure levels (ranging from 2.5-20 mWc), and in which healing took place simultaneously with the permeability test. Their findings indicate that specimens subjected to lower water pressures while healing exhibited improved healing rates. Similar setups working at high (~20 mWc) have also been used later on in the literature (7). In the case of test setups working at low water pressures, other authors (11, 12) used a method based on sealing PVC ring and applying a water-filled tube system with a water pressure of around 0.3 mWc. In this case, the water permeability is evaluated as the reduction of water height in the pipette. In the end, the test selection should depend the application and objectives.

Ultra-High-Performance Fiber Reinforced Concrete (UHPFRC) is a cementitious material that combines self-compacting behavior with excellent mechanical, and durability properties, and shows high ductility and tensile strength (13). Its excellent properties are attributed to a dense matrix, low w/c and high content of micro steel fibers (14). UHPFRC mixes with high contents of fibers and appropriate mix design may have multiple cracking behavior, thanks to a high stress redistribution that produces several narrow microcracks. The porosity accessible to water in UHPFRCs without cracks at 28 days can be 7 and 4 times lower than a 30 MPa and a 90 MPa concrete, respectively (15, 16).

Previous studies (17) investigated UHPFRC beams loaded with increasing levels of strain in order to produce multiple cracks, representing service and failure conditions. A threshold was detected around the residual strain of 1.3‰, if strains were lower, no differences were detected in the water permeability coefficient of UHPFRC. This value of strain was approximately equivalent to a total crack width of around 130 μm distributed in 100 mm. Similarly, previous research in cracked conditions with 20 mWc water pressure (16) could not detect water movement through 25 μm cracks, and only extremely low movement for 50 μm cracks. As a result, a modified water permeability test was developed (17, 18), using sodium chloride and its reaction with silver nitrate as an indicator to identify areas where water could penetrate.

The lack of water flow reported in (17, 18) can be a consequence of the cracking methodology in reinforced beams, which makes the crack width to be reduced towards the interior of the beam, typically in a "V" shape. However, other methodologies, such as those proposed in COST Action Sarcos (19) used concrete disks cracked by splitting tests with completely passing cracks in most of the specimens. Therefore, this study aims to compare the autogenous healing capability of UHPFRC with two fiber types and dosages, through crack closure and water permeability. In addition, protection against chloride penetration after healing was evaluated in disks with completely passing cracks after healing.

2. MATERIALS AND METHODS

2.1. Materials

The study compares two different Ultra High-Performance Fiber Reinforcement Concrete (UHPFRC) mixtures. In order to assess the effect of fiber content on self-healing properties, these mixtures were modified to incorporate varying types and amounts of fiber. The components used in the UHPFRC mixes included Lafarge's CEM I 42.5 R-SR5, Elkem's silica fume, silica sand (0/0.5 mm and 0/1.6 mm), silica flour (Quarzfin U-S 500) from Sibelco. Regarding the fibers, the U160 mix contained high strength short, straight steel fibers, specifically 13/0.2 (length 13 mm, diameter=0.2 mm, slenderness=65), with tensile strength greater than 2000 MPa. The U40 mix incorporated 65/35 3D steel fibers from Dramix (length =35 mm, diameter =0.55 mm, slenderness =65). Fibers were added as reinforcement material, without changing the content of the other compounds. The superplasticizer Sika Viscocrete 20HE was added to both mixtures to ensure self-compacting behavior. Detailed compositions of the two concrete mixes are presented in Table 1. To validate the results acquired from this study, the results from previous studies have been compared, U160 (same mix) and U130 from the results presented in (18) and U120 for the results test-

Table 1. Composition of the four UHPFRC mixes compared.

Materials (kg/m^3)	U160	U40	U130(*)	U120(*)
CEM I 42.5 R-SR5	800	800	800	600
Silica fume	175	175	175	
Slag				500
Silica sand (0/0.5 mm)	302	302	302	
Silica sand (0/1.6 mm)	565	565	565	
Silica flour	225	225	225	
Sand (0-2)				982
Water	160	160	160	200
ViscoCrete 20HE	30	30	30	
Superplasticizer BASF Glenium ACE 300®				33
Short steel fibers (13/0.2)	160	-	130	
Steel fibers Azichem Readymix 200®				120
Dramix fibers 65/35	-	40	-	
w/c	0.20	0.20	0.20	0.30
w/b	0.16	0.16	0.16	0.18

ed by the authors included results in (20). The composition of these UHPFRCs is also presented in Table 1, and are indicated with an (*).

Each mix was evaluated by measuring its compressive strength at 28 days, following the EN 12390-3 standard. This involved testing four cubes for each mix, each cube having a side length of 100 mm. The slump flow test was also conducted to assess workability following EN 12350-2. The compressive strength results at 28 days show that the U160 samples achieved 140.52 MPa, while the U40 samples reached 123.0 MPa (14% improvement due to the fibers). Regarding the slump flow measurements, U160 exhibited a slump flow of 560 mm, whereas U40 showed a higher slump flow of 610 mm. Although the higher fiber content slightly reduced workability, both mixes remained self-compacting and fell within the SF1 slump class (with a slump flow ranging from 550 to 650 mm).

To evaluate the self-healing properties of the mixes, eight cylinders of each mix were prepared, with dimensions of Ø100×200 mm. After curing for 28 days in a humidity chamber set at 20ºC and 95% RH, the cylinders were cut into smaller disks of size Ø100×50 mm. The methodologies used for testing adhered to the guidelines of the COST Sarcos Interlaboratory test groups (19, 20).

2.2. Methodology

2.2.1. Pre-cracking and crack width measurement

To assess the self-healing capability of the four mixes, 28-day-old disks with dimensions of Ø100×50 mm were pre-cracked using a splitting test. During the pre-cracking process, the load increased progressively and crack width in the loaded state was measured manually. Once the crack reached the desired size, the specimens were unloaded and the residual crack width was evaluated. The fibers added to the mixes allow controlling the cracking process until the target crack width is achieved. In this work the goal was to create residual cracks ranging between 100 and 450 µm. The width of these cracks was measured the same day after pre-cracking and then again after the samples healed under various conditions. For every healing condition, at least six specimens were cracked.

The crack width was measured at six points on each disk (three equidistant points on each plane surface). The measuring points are marked yellow (see Figure 2). The results show that 100% of the cracks on the U40 disks were single cracks without (or with minimal) branching, as shown in Figure 2 (left). Conversely, 70% of the measurement points on the U160 disks had several crack branches, *i.e.* a multi-cracking pattern. Therefore, more than one crack was present at most of the measurement points (Figure 2, right).

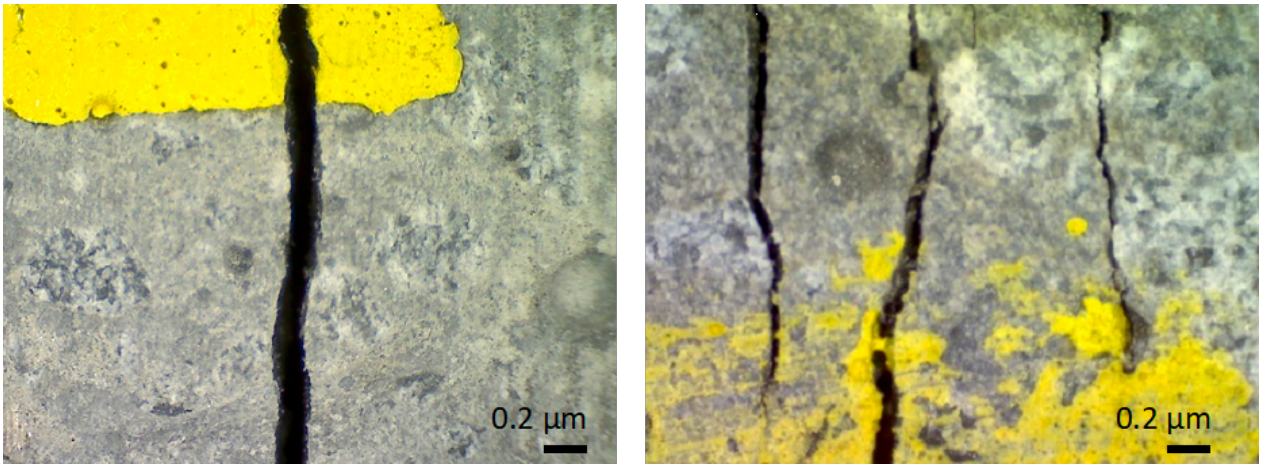

Figure 2. Single crack produced in the U40 mix (left) and several branches in U160 mix (right).

Since crack width was measured in all the individual cracks before and after healing, the parameter of crack closure was evaluated for each individual crack. However, as water and chloride permeability tests were conducted on the entire disk, each disk's representative initial crack width was calculated. To obtain this representative value, the crack width at each measurement point was determined by summing the widths of all the crack branches at each point. The overall representative crack width for the disk was then calculated as the average of all the width measurements from the six points.

2.2.2. Evaluation of the self-healing efficiency

Two parameters were used for the evaluation of self-healing efficiency: the crack Closure Ratio (CR) and the Healing Ratio (HR). CR is obtained using the crack width values of each individual crack width before and after the healing process (Equation [1]). HR is obtained from the low pressure water permeability tests results, performed on cracked disks following the methodology explained in detail in previous studies (8). HR was obtained as the ratio of water permeability, before and after the healing process, following Equation [2].

$$CR=1-\frac{\textit{Crack width after healing}}{\textit{Crack width before healing}} \quad [1]$$

$$HR=1-\frac{\textit{Water head reduction after healing}}{\textit{Water head reduction before healing}} \quad [2]$$

Afterwards, specimens are exposed to the healing condition: a) W28, 28 days of water immersion at 20°C, and H28, 28 days at 20°C and 95% RH.

2.2.3. Protection against chloride penetration

After the healing period under the two healing conditions and the completion of the final water permeability test, an assessment of chloride penetration through the healed cracks was performed. The method used was a modified chloride permeability test, as proposed in a previous study (18). The results of this method revealed two main penetration zones: penetration through the matrix, labeled P_0 and penetration through the crack, labeled W. To measure P_0, four points were marked at 20 mm intervals along both faces of the disk. To measure W, three points were measured, maintaining a 20 mm distance from the surface of exposure to chlorides, in order to avoid the influence of matrix penetration.

3. RESULTS AND DISCUSSION

3.1. Crack closure

Figure 3 and Figure 4 show Crack Closure Ratio (CR) obtained after healing, depending on the initial crack width of each individual crack for both the U160 mix (blue points), U40 mix (orange points). Figure 3 shows the results healing in water immersion for 28 days (W28) and Figure 4 those healing in humidity chamber for 28 days (H28).

Disks from the U160 mix showed distributed cracking with a higher number of thinner cracks, therefore, the CR parameter was analyzed in a higher

number of cracks in the U160 mix. U160 mix had perfect CR in the W28 conditions for most cracks below 360 µm. However, some cracks remained open with CR=0. When U160 disks heal in the H28 conditions, the CR result is dispersed and below 63% in most of the cases, with only two cracks with perfect CR (100%). In the case of the U40 mix healed in W28, it showed several cracks with perfect healing, some cracks with disperse healing between 6 and 60% healing and some cracks that remained completely open CR=0. In the case of U40, healing in H28, the cloud of values obtained is between 0 and 84%, and none of the cracks had perfect healing. Comparing these results with the literature (20), the mix U120 had most cracks with a lower initial width, around 100 µm, and they obtained a wide dispersion of crack closure ratios, with most of the values above 60%. Other research analyzing UHPFRC with very thin cracks (21), below 20 µm, had dispersed values between 60 and 90%, for specimens healing in humidity chamber for 28 days and over 70% for specimens healing in geothermal water.

3.2. Water permeability

Figure 5 shows HR depending on the initial crack width and the healing condition. The water permea-

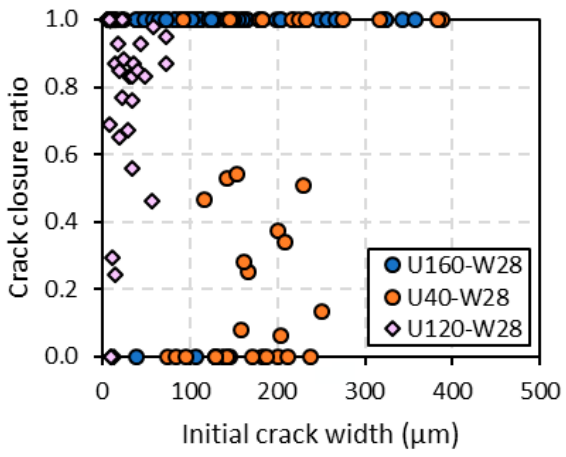

Figure 3. Crack closure ratio vs. initial crack width for every crack of specimens healed in water immersion for 28 days.

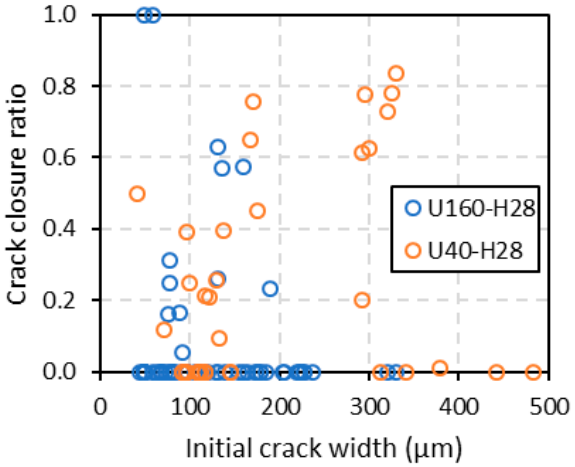

Figure 4. Crack closure ratio vs. initial crack width for every crack of specimens healed in humidity chamber for 28 days.

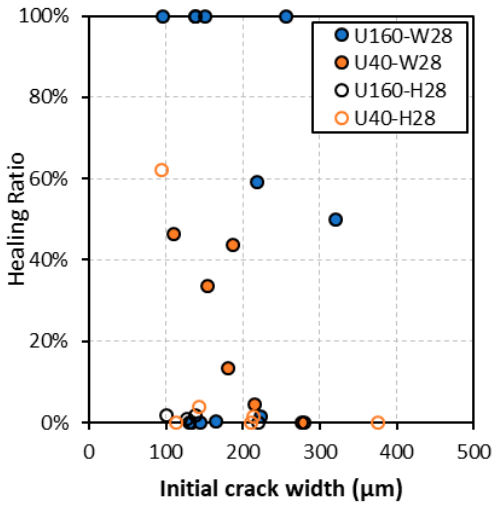

Figure 5. Crack healing ratio for every disk vs. the average initial crack width of the disk.

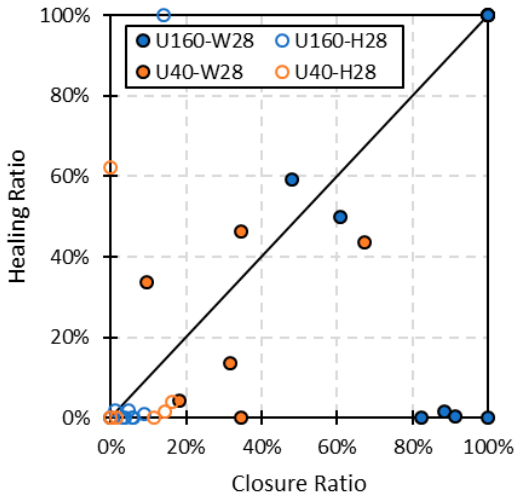

Figure 6. Healing ratio vs. crack closure ratio depending on the fiber content and healing condition.

bility test was conducted on the entire disk, therefore, a representative crack width was calculated for each disk as the initial crack width value. The results show that U160 had improved healing when healed in W28, or disks with a representative crack width of less than 150 μm. However, disks with wider cracks displayed more variable results, and some disks obtained HR values of zero. In the case of the mix U40, the results are below 50% even for disks with representative cracks below 100 μm when healing in W28 and below 10% when healing in H28.

Most published studies focus on healing through one parameter, but information on how the different healing indices compare offers meaningful insights into the long-term durability of structures. Figure 6 compares global crack closure of each specimen (average of all the cracks) with its healing ratio. Specimens healed in water immersion are generally aligned in the bisecting line (CR=HR) or they are U160 specimens with high CR ratio and low HR ratio. Specimens healed in humidity chamber are mainly gathered in the area of almost zero CR and almost zero HR. This observation indicates is consistent with findings from previous studies (18), which suggest a direct correlation between crack closure and healing ratios when healing occurs under water immersion conditions. In addition, the lower values of global crack closure when compared with the individual crack closure of single cracks, indicate that healing may occur at specific locations of an element without improving its overall behavior. Other works on UHPFRC (21) also showed good correlation comparing these two types of self-healing with most of the results placed on the bisecting line.

3.3. Chloride penetration in healed cracks

Even though the crack closure and healing ratios for U160 healed in water immersion (W28) were almost 100%, the chloride penetration patterns indicated that chlorides still managed to penetrate through the cracks to some extent, regardless of whether they exhibited single or multiple cracking patterns. Figure 7 shows the cracking and chloride penetration patterns revealed by silver nitrate pigmentation.

Regarding the parameter of matrix penetration (P_0), the results indicated that the U160 mix had 0 mm or not detectable penetration, regardless of the healing condition. This lack of penetration was also observed in uncracked reference disks. These findings are consistent with previous literature publications (18), which reported complete resistance to matrix penetration in UHPFRC containing 160 or even 130 kg/m³ of short steel fibers after healing in water immersion condition. On the other hand, the P_0 values for the U40 mix were higher, despite having the same UHPFRC matrix composition. The results of penetration when healing in water immersion were an avg. of 0.92 mm (std. dev. 1.14 mm), while those healed in the humidity chamber had an avg. P_0 of 2.48 mm (std. dev. 2.52 mm).

Figure 8 presents the results of W, the depth of chloride penetration through the cracks. The U160 disks healed in W28 showed full resistance to chloride penetration, for cracks < 300 μm. In contrast, the W values for U40 disks healed in W28 varied from 4-6 mm for initial crack widths between 100-300 μm. For U160 and U40 disks cured in H28, both mixes showed similar W values ranging from 0-2 mm.

Regarding previous results (18), UHPFRC samples with a same mix composition with 160 or even 130 kg/m³ of short steel fibers, healed in water immersion for 28 days exhibited penetration through the crack (W) between 4 and 6 mm. However, that study also observed some results may have been influenced by contamination introduced by the wet-cutting methods used during the preparation of the samples. Similarly, (20) showed penetration values through the matrix below 6 mm, in a UHPFRC mix with 120 kg/m³.

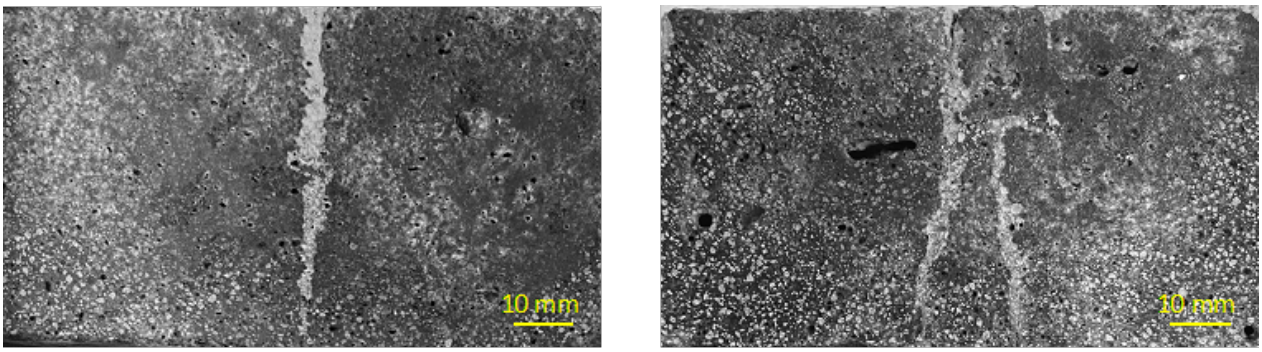

Figure 7. Example of chloride penetration and crack patterns of disks healed in H28, U40 mix (left) and U160 mix (right). Chloride penetration was quantified through the average P0 and W values for each disk under all mixes and healing conditions.

When comparing the W and P_0 values, Figure 9, U40 samples healed in water immersion show values close to the bisecting line, indicating a similar value of the two parameters. U40 samples healed under H28 showed more dispersed W and P_0 values. U160 samples healed under the W28 condition demonstrated complete resistance to penetration of chlorides through both the matrix and the crack path, with values placed in the origin of the graph. However, U160 disks healed in the H28 condition showed crack penetration (W) that did not correspond to matrix penetration, which may be caused by internal multi-cracking and a concentration of micro-cracks.

4. CONCLUSIONS

The results obtained in this study highlight the importance of the presence of fibers, not only for improving the mechanical properties of UHPFRC, but also to improve the durability and self-healing behavior of the material.

On the one hand, the UHPFRC mix with 160 kg/m³ of fibers demonstrated a complete closure of cracks, particularly for initial cracks measuring below 350 µm when healing immersed in water for 28 days. This contrasts with the U40 mix, which displayed a limited crack healing capability, with most cracks closing less than 60%. Under high humidity conditions, both mixes showed reduced crack closure capability, highlighting the need for direct water contact to promote autogenous healing reactions in UHPFRC.

On the other hand, the healing ratio, evaluated by the recovery of impermeability showed that the only mix able to reach complete healing was that with 160 kg/m³ of fibers, and only when healing in water immersion. In addition, this mix also displayed complete resistance to chloride penetration, even for initial cracks up to 300 µm. In contrast, the UHPFRC mixes with lower contents of fiber showed some extent of penetration, around 4 mm in all the cases.

Additionally, it should be noted that crack closure measures might overestimate the self-healing based on water permeability. At the same time, water permeability tests could overestimate the level of protection achieved against chloride penetration.

Authorship contribution statement

Marta Roig-Flores: Conceptualization, Formal analysis, Investigation, Methodology, Supervision, Validation, Writing - original draft, Writing - review & editing.

Hesam Doostkami: Data curation, Formal analysis, Investigation, Methodology, Writing - original draft.

Pedro Serna: Funding acquisition, Methodology, Resources, Supervision, Validation, Writing - review & editing.

Declaration of competing interest

The authors of this article declare that they have no financial, professional or personal conflicts of in-terest that could have inappropriately influenced this work.

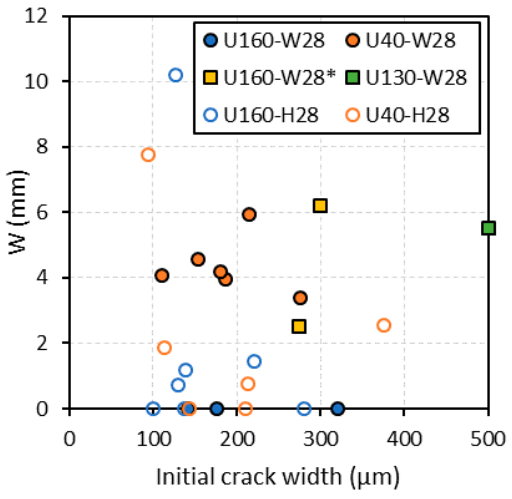

Figure 8. Chloride penetration depth through the crack (W) vs. initial crack width, depending on the mix and healing condition.

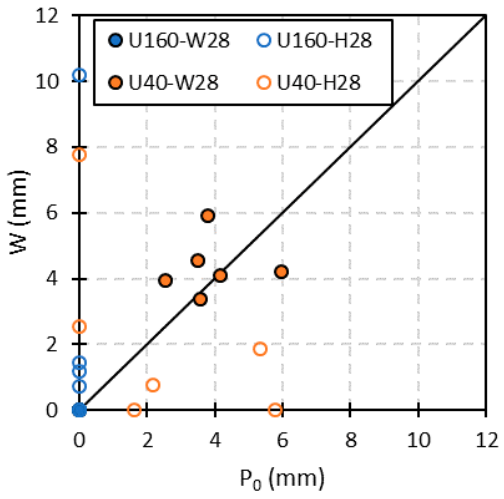

Figure 9. Chloride penetration depth through the crack (W) vs. chloride penetration through the matrix (P), depending on the mix and healing condition.

REFERENCES

1. De Belie N, Gruyaert E, Al-Tabbaa A, Antonaci P, Baera C, Bajare D, Jonkers HM. 2018. A review of self-healing concrete for damage management of structures. Adv. Mater. Interfaces. 5(17):1800074. https://doi.org/10.1002/admi.201800074
2. Lauer KR. 1956. Autogenous healing of cement paste. In Journal Proceedings Vol. 52(6):1083-1098. https://doi.org/10.14359/11661
3. Cánovas MF. 1994. Patología y terapéutica del hormigón armado. Colegio de Ingenieros de Caminos, Canales y Puertos, Servicio de Publicaciones. ISBN 8474932025
4. Edvardsen C. 1999. Water permeability and autogenous healing of cracks in concrete. ACI Materials Journal. 96(4):pp. 448-454). Thomas Telford Publishing. https://doi.org/10.14359/645
5. Ter Heide N, Schlangen E, van Breugel K. 2005. Experimental study of crack healing of early age cracks. Department of Civil Engineering, Technical University of Denmark.
6. Roig-Flores M, Formagini S, Serna P. 2021. Self-Roig-Flores M, Formagini S, Serna P. 2021. Self-healing concrete-what is it good for? Mater. Construcc. 71(341):e237. https://doi.org/10.3989/mc.2021.07320
7. Roig-Flores M, Pirritano F, Serna P, Ferrara L. 2016. Effect of crystalline admixtures on the self-healing capability of early-age concrete studied by means of permeability and crack closing tests. Constr. Build. Mater. 114:447-457. https://doi.org/10.1016/j.conbuildmat.2016.03.196
8. Ferrara L, Van Mullem T, Alonso MC, Antonaci P, Borg RP, Cuenca E, De Belie, N. 2018. Experimental characterization of the self-healing capacity of cement based materials and its effects on the material performance: A state of the art report by COST Action SARCOS WG2. Constr. Build. Mater. 167:115-142. https://doi.org/10.1016/j.conbuildmat.2018.01.143.
9. Neville AM. 1995. Properties of concrete (Vol. 4, p. 1995). London: Longman. ISBN: 978-0-273-75580-7
10. Desmettre C, Charron JP. 2011. Novel water permeability device for reinforced concrete under load. Mater. Struct. 44:1713-1723. https://doi.org/10.1617/s11527-011-9729-6
11. Aldea CM, Shah SP, Karr A. 1999. Effect of cracking on water and chloride permeability of concrete. J. Mater. Civ. Eng. 11(3):181-187. https://doi.org/10.1061/(ASCE)MT.1943-5533.0002050
12. Van Tittelboom, K, De Belie, N, De Muynck, W, Verstraete, W. (2010). Use of bacteria to repair cracks in concrete Cem. Concr. Res. 40(1):157-166. https://doi.org/10.1016/j.cemconres.2009.08.025
13. Habel K, Gauvreau P. 2008. Response of ultra-high performance fiber reinforced concrete (UHPFRC) to impact and static loading. Cem. Concr. Compos. 30(10):938-946. https://doi.org/10.1016/j.cemconcomp.2008.09.001 .
14. Charron JP, Denarié E, Brühwiler E. 2007. Permeability of ultra high performance fiber reinforced concretes (UHPFRC) under high stresses. Mater. Struct. 40:269-277. https://doi.org/10.1617/s11527-006-9105-0
15. VValcuende M, Lliso-Ferrando JR, Roig-Flores M, Gandía-Romero J. M. 2021. Porous Structure of ultra-high-performance fibre-reinforced concretes. Materials. 14(7):1637. https://doi.org/10.3390/ma14071637
16. Sohail MG, Kahraman R, Al Nuaimi N, Gencturk B, Alnahhal W. 2021. Durability characteristics of high and ultra-high performance concretes. J. Build. Eng. 33:101669. https://doi.org/10.1016/j.jobe.2020.101669
17. Negrini A, Roig-Flores M, Mezquida-Alcaraz EJ, Ferrara L, Serna P. 2019. Effect of crack pattern on the self-healing capability in traditional, HPC and UHPFRC concretes measured by water and chloride permeability. In MATEC Web of Conferences 289:1-8. https://doi.org/10.1051/matecconf/201928901006
18. Doostkami H, Roig-Flores M, Serna P. 2021. Self-healing efficiency of Ultra High-Performance Fiber-Reinforced Concrete through permeability to chlorides. Constr. Build. Mater. 310:125168. https://doi.org/10.1016/j.conbuildmat.2021.125168
19. Roig-Flores M, Doostkami H, Alonso MC, Ammar L, Bajare D, Beltran-Cobos R, Serna P. (2022). Evaluation of the self-healing efficiency of concrete with a crystalline admixture: interlaboratory analysis from COST SARCOS RRT3 group.
20. Lo Monte F, Repesa L, Snoeck D, Doostkami H, Roig-Flores M, Jackson S, Blanco Alvarez A, Nasner M, Paul Borg R, Schröfl C, Giménez M, Alonso MC, Serna, P, De Belie N, Ferrara L. 2024. Multi-performance experimental assessment of autogenous and crystalline admixture-stimulated self-healing in UHPFRCCs: Validation and reliability analysis through an inter-laboratory study. Cem. Concr. Compos. 145:105315. https://doi.org/10.1016/j.cemconcomp.2023.105315
21. Cuenca E, D'Ambrosio L, Lizunov D, Tretjakov A, Volobujeva O, Ferrara L. 2021. Mechanical properties and self-healing capacity of Ultra High Performance Fibre Reinforced Concrete with alumina nano-fibres: Tailoring Ultra High Durability Concrete for aggressive exposure scenarios. Cem. Concr. Compos. 118:103956. https://doi.org/10.1016/j.cemconcomp.2021.103956